Development 136, 2265-2276 (2009) doi:10.1242/dev.032938

Orthologs of *Arabidopsis thaliana* stomatal bHLH genes and regulation of stomatal development in grasses

Tie Liu[1], Kyoko Ohashi-Ito[1,2] and Dominique C. Bergmann[1,*]

Stomata are adjustable pores in the plant epidermis that regulate gas exchange between the plant and atmosphere; they are present on the aerial portions of most higher plants. Genetic pathways controlling stomatal development and distribution have been described in some detail for one dicot species, *Arabidopsis*, in which three paralogous bHLH transcription factors, FAMA, MUTE and SPCH, control discrete sequential stages in stomatal development. Orthologs of *FAMA*, *MUTE* and *SPCH* are present in other flowering plants. This observation is of particular interest when considering the grasses, because both the morphology of guard cells and their tissue distributions differ substantially between *Arabidopsis* and this group. By examining gene expression patterns, insertional mutants and cross-species complementation studies, we find evidence that FAMA function is conserved between monocots and dicots, despite their different stomatal morphologies, whereas the roles of MUTE and two SPCH paralogs are somewhat divergent.

KEY WORDS: Stomata, Monocotyledon, Rice, *Arabidopsis*, Maize, bHLH

INTRODUCTION

Plants conquered land approximately 400 million years ago (Edwards et al., 1998). Correlated with this expansion in habitat was the development of an epidermis that, although made highly impermeable by a lipid-rich cuticle, still permitted the exchange of external CO_2 for internal O_2 and water vapor. Microscopic epidermal valves called stomata were the structural innovations that allow this regulated exchange (Edwards et al., 1998). Stomata are present on the aerial surfaces of all large land plants. At a minimum, stomata consist of two guard cells, a pore and an underlying airspace. In many species, however, the stomatal complex includes subsidiary cells adjacent to the guard cells. Both guard and subsidiary cells are morphologically distinct from other epidermal cell types. Since their appearance in the fossil record (contemporaneous with the appearance of land plants), stomatal densities and distributions have changed significantly, but guard cell morphology has remained quite constant (Edwards et al., 1998). In general, there are only two broad classes of stomatal guard cells: the kidney-shaped cells found most plant species and the dumbbell-shaped guard cells found in grasses (Evert, 2006) (see Fig. 1A).

Grass stomata, as described as early as 1881 (Campbell, 1881), have both a pair of dumbbell-shaped guard cells and associated subsidiary cells. Grass stomata are usually arranged in linear files and this final arrangement reflects the developmental process that created them (Fig. 1B). Grass stomata may be on either the top (adaxial) or bottom (abaxial) side of the expanded leaf, but in many species they are preferentially or exclusively abaxial.

Grass guard cell morphology is thought to be derived from the kidney-shaped guard cells found in mosses, ferns, gymnosperms, dicots, and some monocots. For convenience, we will refer to this form as 'dicot'. Dicot stomata often lack subsidiary cells, but they may also have two or more such cells. In contrast to the linear arrangement typical of grass stomata, dicot stomata are scattered on leaf surfaces, a pattern that reflects their 'dispersed' mode of development (Fig. 1B). This distribution pattern is not random, however, and stomatal architecture and patterns are valuable taxonomic characters for both living and fossilized plants (Garland, 1984; Stebbins, 1960).

Developmental pathways for stomata in *Arabidopsis*

In *Arabidopsis*, stomatal development requires a series of asymmetric and symmetric cell divisions in a specialized epidermal cell lineage. Stomatal development is initiated by an asymmetric division in a protodermal cell to produce a small meristemoid and a larger sister cell. The meristemoid is a self-renewing cell and can continue asymmetric divisions. However, it possesses only transient 'stem cell-like' properties and after one to three divisions differentiates into a guard mother cell (GMC). The GMC undergoes a single symmetric division to produce a pair of guard cells (Fig. 1B) (reviewed by Bergmann and Sack, 2007). Stomatal development proceeds roughly in an apical-basal gradient with the more mature stages near the tip, but this is not absolute because sister cells of the stomatal precursors might divide later, intercalating new stomata into areas where stomata previously formed (Fig. 1B). Stomata are formed via similar developmental mechanisms on both the abaxial and adaxial leaf surfaces.

Three of the positive regulators that direct this three-step sequential stomatal development in *Arabidopsis* are the closely related basic helix-loop-helix (bHLH) domain transcription factors FAMA, MUTE and SPEECHLESS (SPCH) (MacAlister et al., 2007; Ohashi-Ito and Bergmann, 2006; Pillitteri et al., 2007). SPCH is expressed in many young epidermal cells and controls the first asymmetric division of protodermal cells to initiate the stomatal lineage (MacAlister et al., 2007; Pillitteri et al., 2007). MUTE is highly expressed in meristemoids and is required for termination of meristemoid stem cell identity and the transition to GMC fate (Pillitteri et al., 2007). Finally, FAMA is expressed in GMCs and regulates the last stage of stomatal development by promoting the symmetric differentiation of a GMC into a guard cell pair (Ohashi-Ito and Bergmann, 2006). FAMA, MUTE and SPCH therefore act as molecular switches controlling major cell fate transitions during stomatal development.

[1]Biology Department, 371 Serra Mall, Stanford University, Stanford, CA 94305-5020, USA. [2]Department of Biological Sciences, Graduate School of Science, University of Tokyo, Tokyo 113-0033, Japan.

*Author for correspondence (e-mail: dbergmann@stanford.edu)

Accepted 24 April 2009

Stomatal development in grasses can be divided into five stages (Stebbins, 1960) (Fig. 1B). Here, stomatal development exhibits a strong spatiotemporal gradient with early stages taking place in the proximal portions of the leaf and guard cells differentiating later in distal regions. In stage one, cell files that are capable of forming stomata are determined (blue shading at leaf base, Fig. 1B). Asymmetric division of cells in these files (stage two, middle leaf section, Fig. 1B) generates GMCs as the smaller daughters. A second asymmetric division then occurs in the cells adjacent to the newly specified GMCs to produce a pair of subsidiary mother cells (SMCs), so at this third stage the guard cell complex consists of a GMC and two subsidiary cells. In the fourth stage, the GMC divides symmetrically into two box-shaped guard cells. During the final stage, guard cells undergo extensive elongation and morphogenetic changes to form the final pair of dumbbell-shaped cells with a central pore between them (red cells at tip of leaf, Fig. 1B) (Sack, 1994).

Despite the differences in stomatal ontogeny, morphology and pattern between monocots and dicots, protein sequences of the key regulatory genes *SPCH*, *MUTE* and *FAMA* are highly conserved between representatives of these two angiosperm divisions. In this study, we identify likely orthologs of *Arabidopsis SPCH*, *MUTE* and *FAMA* in two grass species: rice (*Oryza sativa*) and maize (*Zea mays*). Through mutation, transgenics, and by monitoring gene expression in situ, we demonstrate that there is significant conservation of function of the *FAMA* gene between monocots and dicots. By contrast, although *MUTE* and the two *SPCH* genes maintain some common functions in grasses, they have diverged in their roles and domains of expression.

MATERIALS AND METHODS

Plant growth conditions

Arabidopsis thaliana Columbia ecotype seeds were sterilized and vernalized at 4°C for 3 days before sowing. Plants were grown at 22°C with a 16 hours light/8 hours dark photoperiod. Rice plants were *Oryza sativa spp japonica* cv Nipponbare (X.-W. Deng, Yale University) or mutants from RIKEN (NF7789) or POSTECH (PFG3A-52237.R). After de-husking, surface sterilization and imbibition, rice seeds were germinated on Murashige and Skoog (MS) media in magenta boxes for 12 days before transfer to soil and growth at 22°C with a 16 hours light/8 hours dark photoperiod. Maize plants were *Zea mays* GNN5 (V. Walbot, Stanford University); plants were germinated directly in soil in conditions of 16 hours light/8 hours dark.

Comparative sequence and phylogenetic analysis

DNA and amino acid sequences for rice and maize *FAMA*, *MUTE* and *SPCH1/2* were retrieved by BLAST searches against the GRAMENE database (www.gramene.org/multi/blastview) and TIGR database (http://tigrblast.tigr.org). Protein sequences of FAMA, MUTE and SPCH orthologs were aligned using CLUSTALW (version 7.0.9) software, with manual adjustment using Bioedit to align the bHLH motif and the C terminus. Intron/exon structure and splicing patterns of rice and maize bHLH genes were obtained from the GRAMENE database. Additionally, we searched each protein manually for the presence of additional predicted functional domains using multiple software tools available from PROSITE (http://ca.expasy.org/prosite/). A phylogenetic tree was constructed with the aligned stomatal bHLH protein sequences using MEGA [version 3.0; http://www.megasoftware.net/index.html (Kumar et al., 1994)] with a 1000 bootstrap replicates.

cDNA and genomic DNA constructs and plant transformation

Total RNA was isolated from washed whole 10-dpg rice and maize seedlings using the RNeasy Kit (Qiagen, Valencia, CA, USA). cDNAs were generated by SuperScript III reverse transcriptase (Invitrogen, Carlsbad, CA, USA). The 2.72 kb genomic region including coding sequences for *OsFAMA* was amplified from rice genomic DNA. *OsMUTE* (684 bp) and *ZmMUTE* (618 bp) were amplified from rice and maize cDNA, respectively (for primers, see Table 1). A partial clone of *OsSPCH1* (AK287482) was obtained from the Rice Genome Resource Center (http://cdna01.dna.affrc.go.jp/cDNA/). *OsSPCH2* cDNA was produced by RACE PCR amplification performed according to the manufacturer's (Invitrogen) instructions using OsSP2-1F and OsSP2-1R for the 5′ end, and OsSP2-2F and OsSP2-2R for the 3′ end (for primers, see Table 1). Products from amplifications were cloned in pENTR/D-TOPO (Invitrogen) and sequenced. Overexpression constructs were built by recombining each pENTR clone into the binary vector pH35SGS (Kubo et al., 2005). All constructs were introduced into *Arabidopsis* Columbia ecotype by *Agrobacterium tumefaciens*-mediated transformation (Clough and Bent, 1998). Transgenic T1 plants were selected on agar-solidified MS-containing hygromycin. When possible, T2 lines were analyzed for phenotypes, but severe phenotypes (arrest and sterility) generated by the expression of some transgenes sometimes necessitated the use of T1s.

In situ hybridization

Hybridizations were performed as described (Long and Barton, 1998) with minor modifications. Digoxigenin-labeled RNA probes were directed against the unique N-terminal region of *OsFAMA* (1064 bp), the complete cDNA of *OsMUTE* and *ZmMUTE*, the unique third exon (621bp) of *OsSPCH1* and the N terminus (489 bp) of *OsSPCH2* (for primers, see Table 1). Sense RNA probes were used as negative controls. Stomatal lineage-expressed *OsSCR1* (Kamiya et al., 2003) was used as a positive control.

Rescue experiments with statistical analysis

Pro_{FAMA}*::OsFAMA* was constructed by combining the 2.72-kb *OsFAMA* genomic DNA fragment with the 2.5-kb fragment upstream of *FAMA* gene (Ohashi-Ito and Bergmann, 2006) in pMDC107 (Curtis and Grossniklaus, 2003). The construct was transformed into a *fama-1/+* line by agrobacterium-mediated transformation. Similar strategies to construct *Arabidopsis* regulatory regions driving rice or maize cDNAs were used to test complementation of *mute* and *spch* mutants. For each case, T1 transformant lines were selected for hygromycin resistance. T2s from these plants that segregated mutant phenotypes were selected and examined microscopically. The number of phenotypically wild-type versus mutant seedlings (seedlings devoid of stomata) was counted. These results were analyzed using the χ^2 test from R statistical analysis software. A segregation ratio of 0.25 indicated failure to rescue (reduced to 0.0625 if the construct rescued). All rescue data reported were significant ($P \leq 0.05$) and at least 12 T2 lines were tested for each construct.

RT-PCR to test expression of 35S-driven lines

To test expression levels of *35S::OsMUTE* and *35S::MUTE*, total RNA was extracted using Trizol (Invitrogen) and approximately 500 ng was used in cDNA synthesis reactions using Superscript III Reverse Transcriptase (Invitrogen; for primers, see Table 1).

Microscopy and image processing

Scanning electron microscopy and DIC images were obtained using protocols reported by Ohashi-Ito and Bergmann (Ohashi-Ito and Bergmann, 2006), except that confocal images were acquired using a Leica TCS SP5 confocal microscope. Images were analyzed using ImageJ software and prepared for publication using Adobe Photoshop and Illustrator.

Accession numbers

Sequence data from this article can be found in the TAIR and GRAMENE databases under accession numbers At3g24140 (*FAMA*), At3g06120 (*MUTE*), At5g53210 (*SPCH*), At3g26744 (*SCRM*), At1g12860 (*SCRM2*), Os05g50900 (*OsFAMA*), Os05g51820 (*OsMUTE*), Os06g33450 (*OsSPCH1*), Os02g15760 (*OsSPCH2*), Os11g03110 (*OsSCR1*), Os11g32100 (*OsSCRM1*), Os01g71310 (*OsSCRM2*), AZM5_84542 (*ZmFAMA*), AZM5_28767 (*ZmMUTE*), AZM5_15260 (*ZmSPCH1*) and AZM5_13800 (*ZmSPCH2*).

RESULTS

Arabidopsis stomatal bHLH genes belong to a gene family present in monocots and dicots

Protein sequences of SPCH, MUTE and FAMA are highly similar in the bHLH (putative DNA binding) domain and in an essential C-terminal region (MacAlister et al., 2007) that has previously been

Table 1. Primers for cDNA synthesis, RT-PCR and *in situs*

Name	Primer	Sequence (5′ to 3′)
cDNA synthesis and RT-PCR		
OsFAMA	OsFAMA-F	CACCCACCCCCTGAGTTGGAC
	OsFAMA-R	GTAGTTGACGTCGATGAAGCTAAG
OsMUTE	OsMUTE-F	ATGTCGCACATCGCCGTGGAG
	OsMUTE-R	GGAATGGAGGTGATTATCGGG
AtMUTE	At-MUTE-F	GAACTCCAGAAGAGAATGTTG
	At-MUTE-R	GATACAGCGTCTAGTACATGTAG
OsSPCH1-SP1	OsSPCH1-1-F	AATCATCAATTCATCATCCATGTC
OsSPCH1-SP2	OsSPCH1-1-R	AGGTTCTCGTTCATCTGCTTCCT
OsSPCH2	OsSP2-1-F	GGTTAGCTTAGCTTAGGTTGTTTGC
	OsSP2-1-R	ACTTGCTGAAGCTCCTTGATGTAAT
	OsSP2-2-F	AGATCAGGCGTCAATCATAGGAG
	OsSP2-2-R	AGAAAGTTTGCTGAATTTCTTGCAC
ZmMUTE	ZmMUTE-F	ATTATGTCCCACATCGCGGTGGAGC
	ZmMUTE-R	TGATTCTCCTCCTGCGGCTTCTGCT
In situ hybrizations		
OsFAMA	OsF-IST4E-F	GTGCAGCAGAGAAGCCACCTGGAGAGA
	OsF-IST4E-R	CTTGACGTTGAAGGAGTAGAGGA
OsMUTE	OsMUTE-F	ATGTCGCACATCGCCGTGGAG
	OsMUTE-R	GGAATGGAGGTGATTATCGGG
OsSPCH1	OsS1-IST3E-F	CGGAGACCAGGCATCCATC
	OsS1-IST3E-R	CTTGACAGTGAAGGAGTTGACG
OsSPCH2	OsS2-IST1E-F	ATGGCGGACGGCGGCG
	OsS2-IST1E-R	GTAGAAGCATGGCATGAGCGAGCG
OsSCR1	OsSCR-F	TCCTGCTAACCTCTCCCTCTT
	OsSCR-R	AAAAAGTAAAACCATGTATCCAGTAGA
Genotyping primers		
osfama-1	osfama1-F	ATGATGGATGCTTGGTCTCC
	osfama1-R	GAATTCATCGTCCTCCATCG
osspch2-1	osspch2-1F	TGCCATGCTTCTACGTCAAG
	osspch2-1R	CCTGCACCCACAATTAATAATAC

shown to mediate dimerization in other bHLHs (Feller et al., 2006) (see Tables S1 and S2 in the supplementary material). Despite strong similarity within these two domains, SPCH, MUTE and FAMA each contain unique features, allowing orthologs to be assigned unambiguously. FAMA and SPCH contain N-terminal acidic domains (with limited sequence similarity between them, see Fig. S1 in the supplementary material). This domain in FAMA has been demonstrated to activate transcription (Ohashi-Ito and Bergmann, 2006). SPCH contains an ~90 amino acid domain that is phosphorylated by mitogen activated protein kinases (MAPKs) and is referred to as the MAPK target domain (MPKTD) (Lampard et al., 2008). MUTE encodes neither of these domains (see Fig. S2 in the supplementary material).

To identify homologs of *SPCH*, *MUTE* and *FAMA* within the angiosperms, we searched numerous databases for genomic and EST sequences, concentrating especially on the grasses (GRAMENE; http://www.gramene.org/). Putative orthologs of *SPCH*, *MUTE* and *FAMA* were designated based on protein sequence identity using the entire protein and by comparing intron/exon structures and synteny when possible. Fig. 1C shows a tree of *SPCH*, *MUTE* and *FAMA* sequences from *Arabidopsis*, maize and rice. *FAMA* and *MUTE* are present as single copy genes in these species, whereas two *SPCH* genes are found in each of the grasses (Fig. 1C). The unique features of SPCH, MUTE and FAMA, notably the long N terminus of FAMA and the MPKTD of SPCH are readily apparent in the grass homologs (see Fig. S1 in the supplementary material). Inspection of the genomic microstructures surrounding *FAMA* and *MUTE* indicates a high degree of microsynteny between *Arabidopsis* and rice (Fig. 1D); genes adjacent to *MUTE* and *FAMA* are homologs of the genes adjacent to *OsMUTE* and *OsFAMA*. For example, At3g06140, a ring-finger gene, and At3g06270, a protein phosphatase 2C (PP2C), are adjacent to *MUTE*. In rice, *OsMUTE* is flanked by the ring-finger gene Os05g51780 and the PP2C gene Os05g51510 (Fig. 1D).

Rice *OsFAMA* and maize *ZmFAMA* are highly similar to *FAMA*

The maize and rice genomes each encode a single gene homologous to *FAMA*. *OsFAMA* (Os05g50900) encodes a 493 amino acid protein (see Fig. S1 in the supplementary material). Within the bHLH domain, OsFAMA is 94% (47/50 amino acids) identical to FAMA. The maize ortholog ZmFAMA (AZM5_84542) is 92% identical to *Arabidopsis*, and the identity between OsFAMA and ZmFAMA is 92% (46/50 amino acids; see Tables S1 and S2 in the supplementary material). The grass *FAMA* genes also share with *Arabidopsis FAMA* a single intron within the bHLH domain at a conserved site (not shown). Although there is limited amino acid identity among the N-terminal extensions of the FAMA genes, these regions might serve similar functional roles as both rice and maize FAMA have glutamine- and proline-rich stretches that are typical of transcriptional activation domains (see Fig. S1 in the supplementary material).

Expression of OsFAMA is in differentiating leaves

If rice and *Arabidopsis FAMA* are required for the same developmental transition, then we would expect *OsFAMA* to be expressed in the leaf epidermis during the GMC to GC transition stages. Furthermore, loss-of-function mutations in rice *fama* should

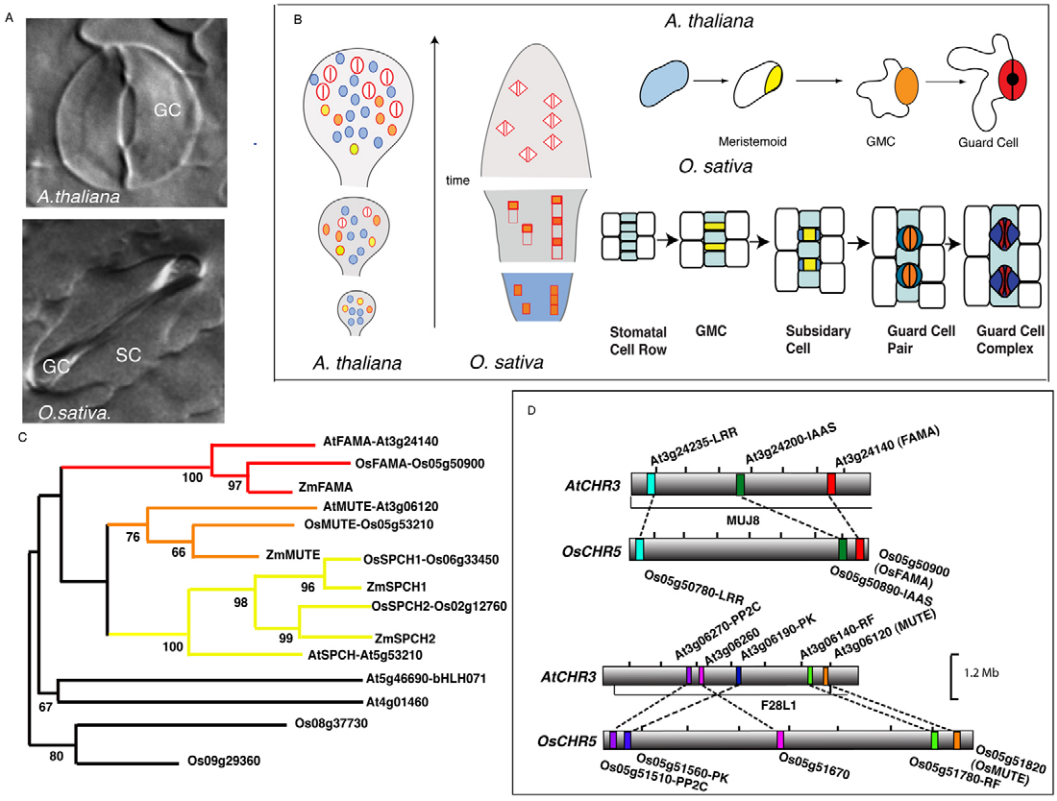

Fig. 1. *Arabidopsis* stomatal bHLH genes and grass orthologs. (**A**) DIC images showing morphology of kidney-shaped stomata in *Arabidopsis* (top) and dumbbell-shaped stomata in rice (bottom). GC, guard cell; SC, subsidiary cell. (**B**) Schematics of stomatal patterning. (Left) Comparison of diffuse (*A. thaliana*) and linear (*O. sativa*) styles of stomatal lineage development (see Croxdale, 2000). In diffuse growth, young leaves contain proliferating cells that initiate stomatal development (blue ovals) and become meristemoids (yellow ovals). Later, the first wave of stomatal precursors pass through GMC fate (orange ovals) and differentiate into stomata (red, bisected ovals), while new cells enter the lineage, intercalating between existing stomata. In monocots, the leaf is strongly zoned; the base is youngest and in this cell proliferation zone (orange boxes, blue region) the files that can later form stomata are established. Later, asymmetric divisions establish GMCs (middle region, orange boxes) and, finally, stomata (tip region, red diamonds). (Right) Details of stomatal lineage cell types. (Top) *Arabidopsis* cell types indicated by color: meristemoid (yellow), GMC (orange), guard cells (red). (Bottom) Rice cell files (light blue) divide to create stomatal precursors, and asymmetric divisions create GMCs (yellow). GMCs induce neighbors to produce subsidiary cells (dark blue), then GMCs divide into a pair of immature guard cells (orange) that undergo morphological change as they mature (red). (**C**) Phylogenetic distribution of stomatal bHLH genes: red, FAMA orthologs; yellow, SPCH orthologs; orange, MUTE orthologs. (**D**) Syntenic regions surrounding FAMA and MUTE in *Arabidopsis* and rice. Syntenic genes are represented by bars of the same color: AtCHR 3, *Arabidopsis* chromosome 3; OsCHR 5, rice chromosome 5; RF, ring finger protein; PK, protein kinase; PP2C, protein phosphastase 2C; IAAS, indole-3-acetic acid-amido synthetase; LRR, leucine-rich repeat. Bars to the right of the FAMA and MUTE represent the corresponding annotated *Arabidopsis* BAC clones.

result in the absence of mature guard cells, while maintaining the normal overall pattern of precursors. RNA in situ hybridization was performed to determine the tissue localization of *OsFAMA*. In wild-type seedlings, *OsFAMA* transcript was first detected in the leaf epidermis and vasculature of the sheath elongation zone (SEZ, Fig. 2B,C). In the leaf blade expansion zone (BEZ, Fig. 2B), *OsFAMA* transcript was most intense in the abaxial epidermis of the sheath (Fig. 2D,E). *OsFAMA* was not detected in the shoot apical meristem (SAM) or in leaf primodia at the earliest stages of leaf development (sheath division zone, SDZ, Fig. 2B,F). This expression pattern is consistent with a gene whose role is to regulate the latest stages of stomatal development.

An insertional mutant of *OsFAMA* exhibits defective stomata

We identified a transposon insertion mutant in OsFAMA (NF7789, Rice Genome Project of NIAS). The *osfama-1* mutant allele harbors an insertion in the third exon (Fig. 3A). We confirmed the presence of the insertion by PCR using primers flanking the insertion site (for primers, see Table 1) and, in homozygous mutants, we did not detect *OsFAMA* transcript (Fig. 2G-I), indicating that *osfama-1* is probably a loss-of-function allele. The homozygous *osfama-1* mutants displayed a severe dwarf phenotype and yellowish leaf blade. At 10 days post-germination (dpg), *osfama-1* homozygotes were only ~30% of the height of their wild-type siblings (Fig. 3B). After transplanting to soil, *osfama-1* plants continued to be smaller than their wild-type or heterozygous siblings, and died before reaching reproductive maturity (Fig. 3C).

The epidermis of the *osfama-1* plants showed an intriguing defect in stomatal development. The linear arrays of stomatal complexes in *osfama-1* mutants were indistinguishable from those of wild type in terms of numbers and overall pattern (Fig. 3D, compare with 3F). However, instead of their typical dumbbell morphology, the two guard cells were box-shaped (Fig. 3E, compare with 3G). Each mature *osfama-1* guard cell resembled a GMC or a very immature wild-type guard cell. We interpret this to mean that *OsFAMA* is

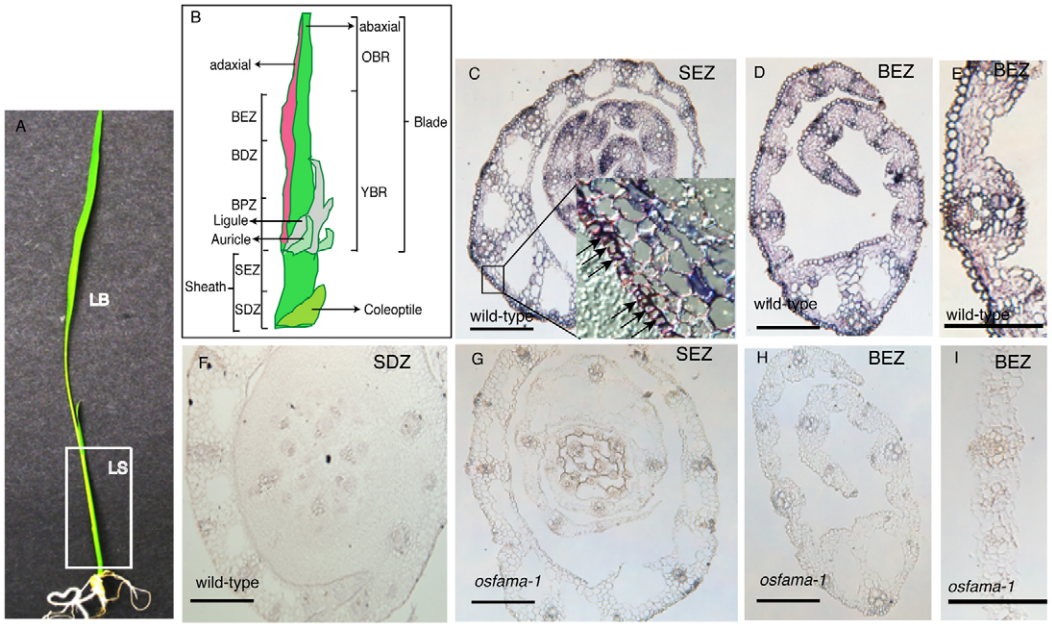

Fig. 2. RNA expression pattern of *OsFAMA* in the vegetative SAM and leaves of rice. (**A**) Photograph of 12-dpg rice seedling; box indicates the region shown schematically in B. LS, leaf sheath; LB, leaf blade. (**B**) Growth zones in the developing rice leaf: SDZ, sheath dividing zone; SEZ, sheath elongation zone; BPZ, blade proliferation zone; BDZ, blade differentiation zone; BEZ, blade expanding zone; YBR, young blade region; OBR, oldest blade region. (**C**,**G**) Cross sections through the sheath elongation zone, showing OsFAMA expression in the leaf sheath epidermis of wild type (C) and but not *osfama-1* (G). Inset in C is a magnified view of the epidermal region, showing strong signal throughout the epidermis (black arrows) (**D**,**E**,**H**,**I**) Cross section through the BEZ, showing the expression in the epidermal tissues in wild type (D; magnified in E), but not *osfama-1* (H; magnified in I). (**F**) Cross section through leaf primordia at the SDZ, showing the absence of *OsFAMA* transcript in this stage leaf primordium. Scale bars: 100 μm in C,D,F-H; 50 μm in E,I.

required for guard cell differentiation. In contrast to the phenotype of *Arabidopsis fama-1* mutants, however, the rice GMCs did not undergo extra cell divisions.

OsFAMA can promote GC differentiation in *Arabidopsis*

Because both *osfama-1* and *Arabidopsis fama* mutants have defects in GC production, but *Arabidopsis* and rice GCs have different morphologies, we tested whether *OsFAMA* could promote the same outcomes as *FAMA* when expressed in *Arabidopsis*. Overexpression of *FAMA* induces the formation of excess, unpaired guard cells in the epidermis of *Arabidopsis* (Ohashi-Ito and Bergmann, 2006). We generated transgenic *Arabidopsis* expressing *OsFAMA* under the control of the cauliflower mosaic virus 35S promoter (*35S::OsFAMA*). Like overexpression of *FAMA* (Fig. 3H), overexpression of *OsFAMA* could induce the production of unpaired guard cells (Fig. 3I), but did so less effectively than *FAMA*. We then expressed *OsFAMA* under the control of the *FAMA* promoter (Pro_{FAMA}*::OsFAMA*) and transformed this construct into heterozygous *fama-1* mutant plants. Among the *fama-1* homozygous mutant progeny from twelve independent T2 transgenic lines, we were able to identify plants with mature guard cells (Fig. 4C). These data indicate that *FAMA* functions to promote guard cell differentiation in representatives of both the monocots and the dicots despite the morphological divergences of stomatal guard cells in these plant groups.

SPCH and *MUTE* expression and function diverge between *Arabidopsis* and monocots

Stages in stomatal development controlled by *SPCH* and *MUTE* in *Arabidopsis* are not easily compared with stages in grass stomatal development. Nonetheless, homologs of these earlier acting bHLHs are readily found. MUTE is a small protein, lacking both an N-terminal extension and a MPKTD (see Fig. S2 in the supplementary material). Homologs from maize and rice are ~80% identical in the bHLH domain and are ~50% identical over the whole protein (see Tables S1 and S2 in the supplementary material). Interestingly, although MUTE is not a predicted or actual substrate of the MAPKs that phosphorylate SPCH (Lampard et al., 2008), OsMUTE and ZmMUTE posses multiple potential MAP kinase phosphorylation sites (see Fig. S1 in the supplementary material). In contrast to the single *SPCH* of the dicots *Arabidopsis*, Poplar and *Ricinus*, SPCH is represented by two genes in rice and maize (Fig. 1C). One of the two rice *SPCH* genes (*OsSPCH2*) is much more similar to *SPCH* than the other (see Tables S1 and S2 in the supplementary material), but all the grass *SPCH* genes are larger than *SPCH*, and the 483 amino acid peptide encoded by *OsSPCH1* is markedly so (see Figs S1 and S2 in the supplementary material). Most of the increased length in OsSPCH1 is in a 190 amino acid N-terminal extension that has little similarity to other SPCH proteins. OsSPCH2 and both maize SPCH paralogs have smaller N-terminal domains containing a conserved transcriptional activation domain. The unique MPKTD region of *SPCH* (relative to *MUTE* and *FAMA*) is easily identified in the grass *SPCH* homologs and the sites demonstrated to be phosphorylated in SPCH are conserved (see Fig. S1 in the supplementary material) (Lampard et al., 2008).

Expression of *SPCH*

We were unable to detect *OsSPCH1* or *OsSPCH2* transcripts in rice tissues from the seedling stage through leaf maturity by in situ hybridization, RT-PCR or RNA blot analysis (not shown). This is not surprising given that SPCH is found at low levels at a transient

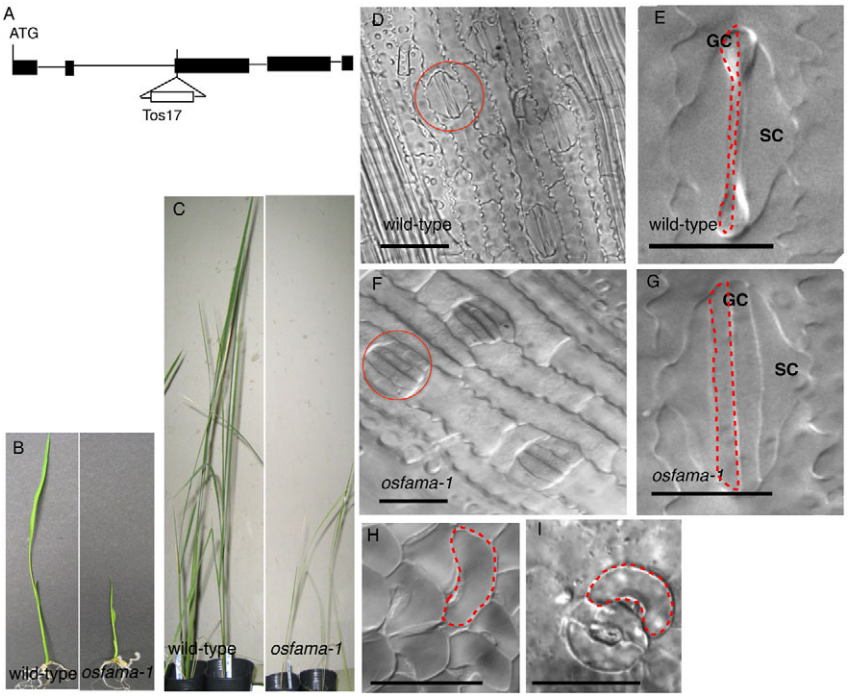

Fig. 3. Phenotypes of *osfama-1*. (**A**) Structure of the *OsFAMA* (Os05g50900) locus and transposon insertion site. (**B**) Phenotypes of wild-type and *osfama-1* mutant plants at 12 dpg, and (**C**) as mature plants. (**D**) Epidermal peel from leaf of wild-type seedling showing characteristic linear arrangement of dumbbell-shaped stomata; red circle indicates a single stoma. (**E**) Enlargement of stoma from D. GC, guard cell; SC; subsidiary cell. Dashed line outlines a single dumbbell-shaped guard cell. (**F**) Epidermal peel from *osfama-1* leaf with normal stomatal arrangement but box-shaped stomata (red circle). (**G**) Enlargement of stoma indicated by the red circle in F; dashed line outlines a single box-shaped guard cell. (**H**) Single-celled stomata (red dashed line) produced by *35S::FAMA*. (**I**) Single-celled stomata (red dashed line) produced by *35S::OsFAMA*. Scale bars: 250 μm in D,F; 20 μm in E,G; 100 μm in H,I.

stage in leaf development (MacAlister et al., 2007). We queried the whole-genome transcriptional profiles of rice cell types isolated by laser-capture microdissection (RICEATLAS, http://bioinformatics.med.yale.edu/riceatlas/search.jspx). *OsSPCH* transcript was detected only in the coleoptile (a covering over embryonic leaves). By contrast, *OsMUTE* and *OsFAMA* were readily detected in multiple young leaf sample tissues, consistent with the in situ data.

Functional assays of SPCH activity

Although we cannot conclude from expression data whether either SPCH homolog is involved in rice stomatal development, we do have recourse to several functional assays – characterization of an insertional mutant in rice, and cross species complementation and overexpression studies. Overexpression of *SPCH* leads to ectopic divisions in pavement cells (MacAlister et al., 2007). No phenotypes were observed with *35S::OsSPCH1* expression, but *35S::OsSPCH2* was able to promote cell division in the pavement cells (see Fig. S3 in the supplementary material). We next tested the ability of *OsSPCH2* (the paralog with activity in the overexpression assay and with higher overall similarity to *SPCH*) to rescue *spch*; however, Pro_{SPCH}*::OsSPCH2* plants failed (0/16 lines) to rescue the *spch* mutant phenotype.

POSTECH insertion mutant lines of *osspch1* (PFG_1D-04011.R) and *osspch2* (PFG_3A-52237.R) were obtained, and we could confirm the presence of an insertion in the *osspch2-1* line (Fig. 5A; for primers, see Table 1). Plants homozygous for the *osspch2-1* insertion were green, but slightly smaller in size than their wild-type siblings (data not shown). Microscopic examination of the leaves revealed an appreciable decrease in the number of stomata (Fig. 5C,D) and the presence of stomatal patterning abnormalities (Fig. 5F). This phenotype is found only in the plants homozygous for the insertion (2/15). Taken together, the functional assays suggest that *OsSPCH2* plays a role in promoting the early events of rice stomatal development, but is not completely equivalent to *SPCH*.

Expression of *MUTE*

By in situ hybridization, *OsMUTE* mRNA first accumulates as rice leaf primordia initiate (Fig. 6B,C). In sections nearest to the base of the leaf, strong expression was observed in the whole P1 primordium, and weak expression was occasionally detected in the P4 leaf (Fig. 6D). In sections that include P1 primordia that enclose

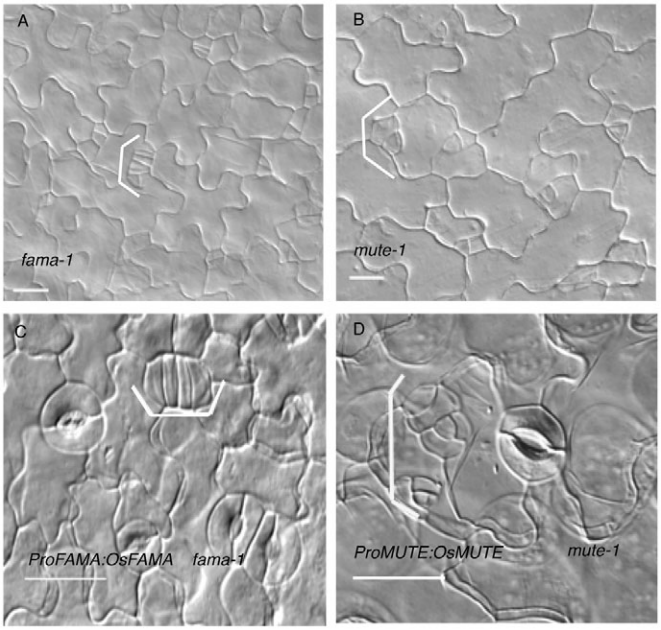

Fig. 4. The FAMA and MUTE rice orthologs complement the corresponding *Arabidopsis* mutants. DIC images of 12-dpg cotyledons. (**A**,**B**) Loss-of-function phenotype of *fama-1* (A) and *mute-1* (B). (**C**) Partial complementation of *fama-1* by Pro_{FAMA}*:OsFAMA*; remaining tumor is indicated (bracket). (**D**) Partial complementation of mute-*1* by Pro_{MUTE}*:OsMUTE*; remaining arrested meristemoids are indicated (bracket). Scale bars: 100 μm.

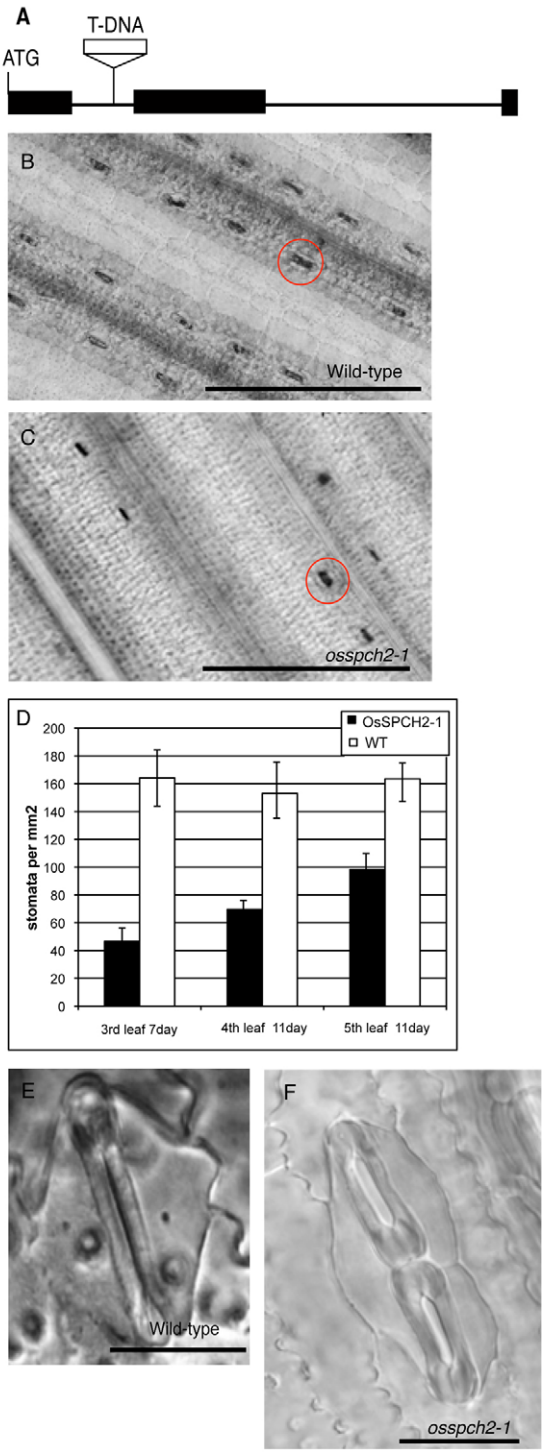

Fig. 5. Phenotypes of *osspch2-1* mutants. (**A**) Structure of the *OsSPCH2* (Os02g15760) locus and the T-DNA insertion site. (**B**) Cleared leaf epidermis showing reduced stomatal density compared with wild type (**C**); red circles indicate stomata. (**D**) Quantification of the stomatal density phenotype. (**E**,**F**) Higher magnification images showing the occasional (<10% of complexes, *n*=200) defect in *osspch2-1*: adjacent GC pairs flanked by a single subsidiary cell on one side and two on the other. Scale bars: 200 μm in B,C; 20 μm in E,F.

the SAM, *OsMUTE* remains strongly expressed in the P1 primordia; in addition, strong expression was also found in the SAM proper and in P2 primordia (Fig. 6E). Transcript accumulates much more strongly in stomatal precursor cells as the P2 leaves mature, whereas the P1 leaves maintain strong expression in all epidermal cells (Fig. 6G). When compared with *OsFAMA* (e.g. Fig. 2B), it is clear that *OsMUTE* is expressed at earlier developmental stages.

OsMUTE expression in rice leaf primordia is spatially and temporally distinct from that in *Arabidopsis*. To test whether this reflected differences in the cis-regulatory elements of the *MUTE* promoters or differences in other factors (different plant morphologies or trans-acting regulatory factors), we made a Pro_{OsMUTE}*::GUS* reporter (for primers, see Table 1). In 20 independent T2 lines we observed Pro_{OsMUTE}*::GUS* activity broadly at young stages in the developing *Arabidopsis* leaf primordia (see Fig. S4B in the supplementary material). GUS staining was also observed in the stomatal lineage cells, but it was not restricted to meristemoids (see Fig. S4C in the supplementary material). This expression pattern differs from that of Pro_{MUTE}*::GUS*, whose expression is observed first at cotyledon tips (Pillitteri et al., 2008), and is then restricted to meristemoids (Pillitteri et al., 2007). The Pro_{OsMUTE}*::GUS* expression in leaves resembles the broad early expression pattern of Pro_{SPCH}*::GUS* (MacAlister et al., 2007).

OsMUTE can complement *mute-1*

We tested whether *OsMUTE* could complement *mute* by expressing *OsMUTE* cDNA with the endogenous *MUTE* promoter or the 35S promoter. *OsMUTE* expressed under either promoter could partially rescue *mute*, as evidenced by altered segregation ratios in the self progeny (see Materials and methods) and by the presence of guard cells at the edges of leaves exhibiting the typical *mute* phenotype (arrested meristemoids) in the center (Fig. 4D).

Overexpression phenotypes of *OsMUTE* in *Arabidopsis*

In *Arabidopsis*, overexpression of *MUTE* leads to the conversion of epidermal cells to GMCs that then divide to form paired guard cells (MacAlister et al., 2007; Pillitteri et al., 2007). We overexpressed *OsMUTE* (*35S::OsMUTE*) in *Arabidopsis* and compared overexpression phenotypes with those produced by *35S::MUTE*. In both cases a spectrum of phenotypes was observed (Fig. 7); the phenotypical disruptions correlated with the level of overexpression, as assayed by RT-PCR (Fig. 7A,I; OL1, OL2 and OL3 of *35S::OsMUTE* transgenic lines and AL1, AL2 and AL3 of *35S::MUTE* plants). At the highest expression levels (AL3 and OL3 lines), both *MUTE* and *OsMUTE* converted all epidermal cells in the cotyledons and leaves into guard cells (Fig. 7H,L). These lines suggest that *OsMUTE* is capable of inducing the same phenotypes as *MUTE* when expressed at very high levels.

The epidermis of lines expressing lower levels of *OsMUTE* looked qualitatively different than lines expressing *MUTE* at comparable levels (Fig. 7A,I). By quantifying the type and number of cells produced by either construct, we found that both could increase total epidermal cell number above that of wild type, but there was a significant difference in the types of cells produced in each case (see Fig. S5 in the supplementary material). Moderately expressed *35S::MUTE* (AL2, Fig. 7C) induced the formation of large guard cell clusters (Fig. 7K) among a few normal jigsaw-shaped pavement cells. By contrast, moderately expressed *35S::OsMUTE* (OL2) led to the production of small, non-stomatal marker-expressing cells at the expense of pavement cells (Fig. 7O). We observed the same trend in epidermal phenotypes in lines with low expression levels of *35S::MUTE* (AL1) and *35S::OsMUTE* (OL1; see Fig. 7B,N,P; see also Fig. S5 in the supplementary material).

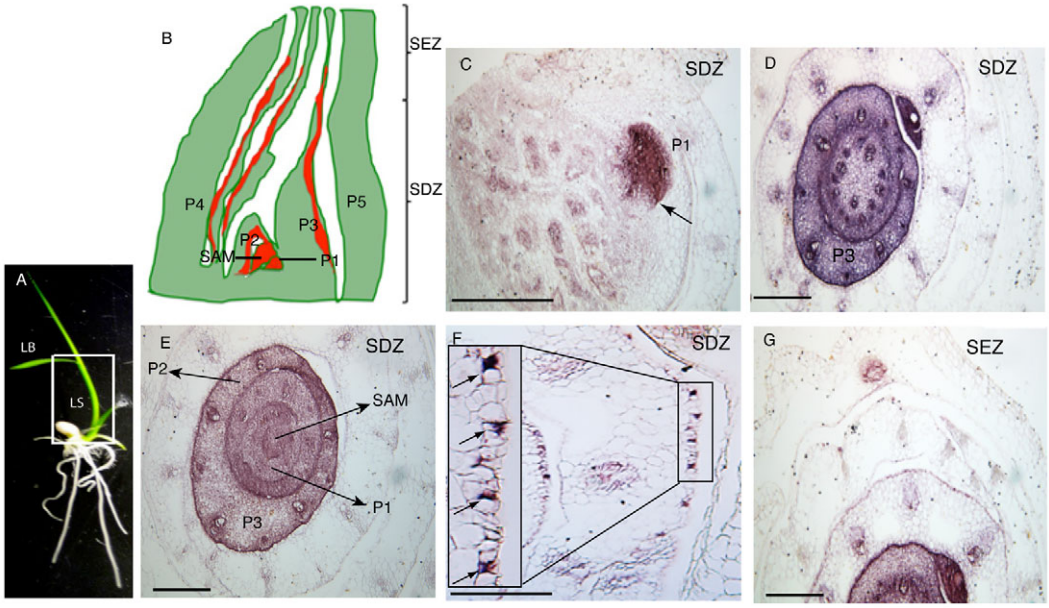

Fig. 6. RNA expression pattern of *OsMUTE* in early rice leaf development. (**A**) 5-dpg wild-type rice seedling with region represented in B boxed. LS, leaf sheath; LB, leaf blade. (**B**) Schematic of rice meristem to illustrate sections probed in C-G. (**C-G**) Brightfield images of transverse sections hybridized with *OsMUTE* probes; relative positions are indicated in B. (C) Cross section through the vegetative rice apex (5-dpg). *OsMUTE* is expressed in the domain of P1 primordium. (D) Cross section through the vegetative rice apex at an older stage (7-dpg), showing expression in P3 leaf. (E) High expression found in the SAM, P1, P2, P3. (F) Higher magnification of mature P2 leaf epidermis, showing strong expression in stomatal precursor cells (arrows). (G) Higher magnification of P2 leaf epidermis; *OsMUTE* is highly expressed in epidermal cells. Scale bars: 50 μm in C-F; 100 μm in G.

35S::OsMUTE effects in a *spch* background

Moderate expression of OsMUTE induces cell division, but the resultant cells do not all become guard cells, a phenotype that is strikingly similar to the phenotypes created by the expression of SPCH variants with altered MPKTDs (Lampard et al., 2008). We examined this connection between OsMUTE and SPCH by expressing OsMUTE in an *spch-3* (null) background. This enabled us to assay the rescue of *spch* by OsMUTE and to carefully characterize the effects of OsMUTE expression in an epidermis lacking stomatal lineage cells (Fig. 8A). *35S::MUTE; spch-3* plants (four independent T2 lines) produced pavement cells and clusters of mature stomata (Fig. 8B) (Lampard et al., 2008). By contrast, *35S::OsMUTE; spch-3* homozygotes from five independent T2 lines exhibited a common phenotype of ectopic epidermal cell divisions. In mature (12-dpg) cotyledons from these lines, the typical crenulated pavement cells were replaced by small cells, but no stomata were produced (Fig. 8C).

Expression pattern and function of the maize *MUTE* homolog

Because *OsMUTE* and *MUTE* did not behave in the same way, and because no insertion mutations in OsMUTE could be verified, we expanded our investigation into the behavior of grass MUTE genes by analyzing MUTE from maize. By RNA in situ hybridization, *ZmMUTE* was expressed in the SAM and in emerging leaf primordia (Fig. 9C-G), with the highest transcript levels in the leaf margins of P1-P4 (Fig. 9G). This expression pattern – strong in immature, mitotically active leaf zones – is similar to that of *OsMUTE*. However, at later developmental stages, *ZmMUTE* RNA expression is broader than that of *OsMUTE* (Fig. 9E, compare with Fig. 6F). Like *OsMUTE*, the *ZmMUTE* cDNA driven by the endogenous *MUTE* promoter (Pro_{MUTE}*::ZmMUTE*) can complement *Arabidopsis mute-1* (12 T2 lines, see Materials and methods).

ZmMUTE induces guard cell production in *Arabidopsis*

In *Arabidopsis*, *35S::ZmMUTE* expression resulted in both stomatal and whole plant phenotypes (Fig. 10A-D). *35S::ZmMUTE* was exceedingly effective at promoting stomatal formation (Fig. 10B-E). The effects on stomatal production were similar to those caused by the strongest lines of *35S::MUTE* (MacAlister et al., 2007; Pillitteri et al., 2007); however, the effect on seedling morphology was unique. Because *35S::ZmMUTE* phenotypes were seedling lethal, we also generated estrogen-inducible lines (Pro_{Est}*::ZmMUTE*). Seedlings germinated on MS plates and transferred at 12-dpg to media containing 5 μM estrogen for 12 hours showed excess cell proliferation (visible after 24 hours, Fig. 10F) and stomatal production (after 48 hours, Fig. 10G; 72 hours, Fig. 10H). It appears that *ZmMUTE* behaves much like *MUTE* in its ability to convert many cell types (including non-stomatal lineage cells) into guard cells.

DISCUSSION

FAMA function is conserved between *Arabidopsis* and rice

Our data provide the first functional evidence that homologs of stomatal genes identified in *Arabidopsis* can regulate stomatal formation in the grasses. *OsFAMA* is closely related to the *Arabidopsis FAMA* gene in sequence and expression pattern, and complements the *Arabidopsis* mutant. Both *fama-1* and *osfama-1* mutants fail to complete the final stage of stomatal formation.

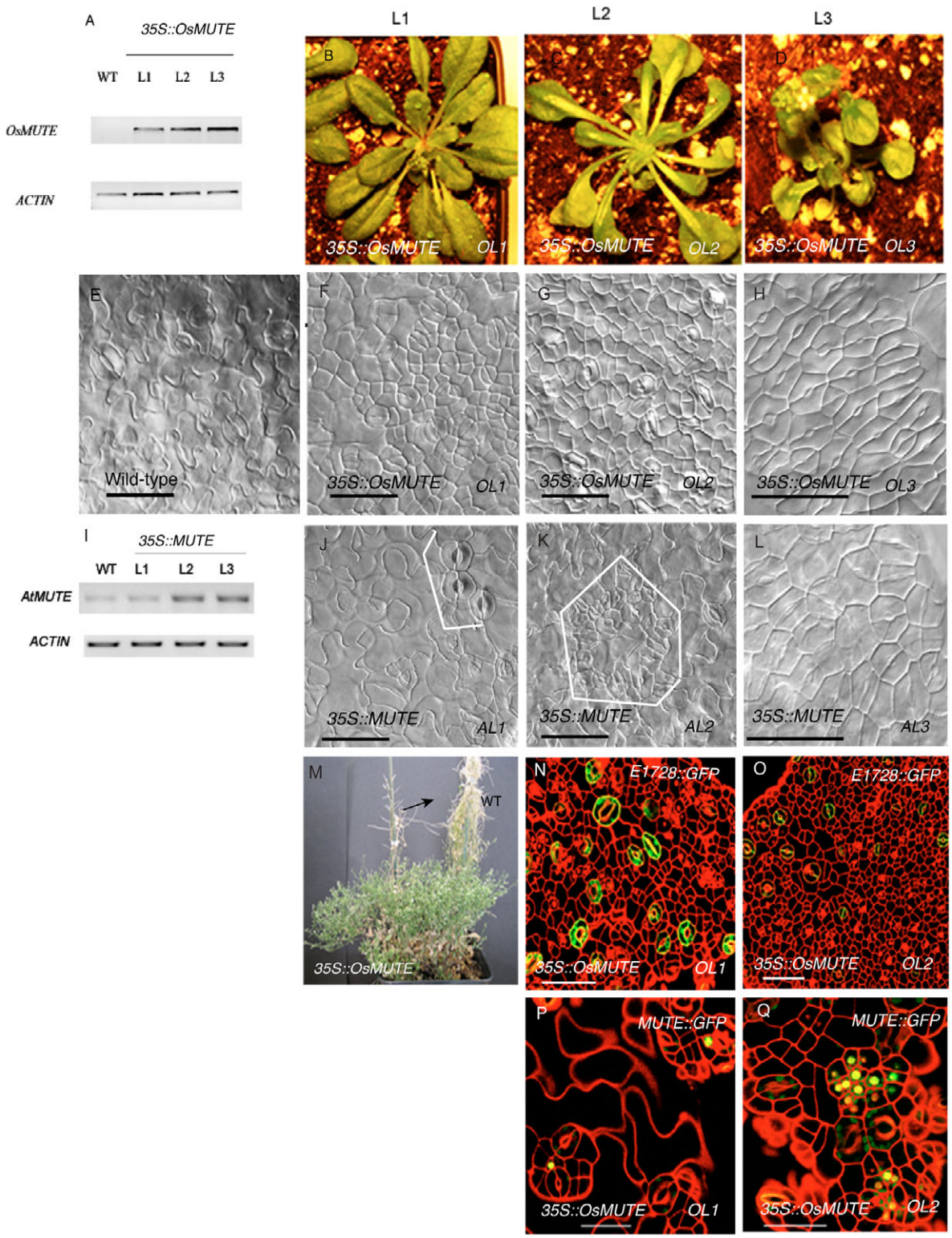

Fig. 7. Phenotypical comparsion of *Arabidopsis 35S::MUTE* and *35S::OsMUTE* overexpression lines. (**A**) and (**I**) RT-PCR analysis of expression levels of *35S::OsMUTE* (OL1, OL2, OL3) and *35S::MUTE* (AL1, AL2, AL3) cDNA (25 cycles), and *Actin* cDNA (30 cycles). (**B-D**) *35S::OsMUTE* plants with mild (OL1), moderate (OL2) or severe (OL3) phenotypes. (**E-H**) DIC images of stomata patterns in *Arabidopsis* cotyledons of wild-type (E), OL1 (F), OL2 (G), and OL3 (H) plants. (**J-L**) DIC images of AL1, AL2, and AL3 stomata phenotypes in *Arabidopsis* cotyledons with mild (J), moderate (K) or severe (L) phenotypes, respectively. White brackets or outlines in J and K indicate stomatal clusters. (**M**) Whole plant phenotype of 3-month-old *35S::OsMUTE* (OL2) plant showing bushy growth habit and reduced fertility compared with wild-type siblings. (**N-Q**) Confocal images of cotyledons counterstained with PI (red) to visualize cell outlines. (N,O) Cotyledon of *35S::OsMUTE* of OL1 (N) and OL2 (O) expressing the mature guard cell marker E1728::GFP (green). (P,Q) Expression of MUTE::GFP (green) marks meristemoids in the cotyledon of OL1 (P) and OL2 (Q). Scale bars: 50 μm in E-G,J-K,N-Q; 80 μm in H,L.

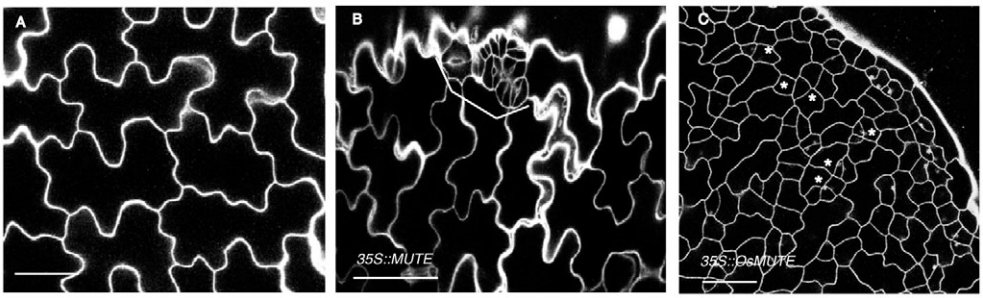

Fig. 8. Phenotypes of *35S::OsMUTE* in *spch*. (**A-C**) Confocal images of 12-dpg seedlings; cell outlines visualized by PI staining (white). (A) Cotyledon epidermis of *spch-3* showing only interlocking pavement cells. (B) *35S::MUTE; spch-3* plants, showing clustered guard cells (bracket). (C) *35S::OsMUTE; spch-3*, showing extra division of pavement cells (asterisks). Scale bars: 50 μm.

These findings suggest that the bHLH transcription factor *FAMA* acts at a high level in a transcriptional regulatory cascade – in essence specifying the transition to guard cell fate, not the details of guard cell morphology. This role is consistent with previous reports that ectopic expression of *FAMA* could override previous differentiation status and induce guard cell characteristics in root epidermal and leaf internal mesophyll cells (Ohashi-Ito and Bergmann, 2006).

Although there is conservation between the functions of *Arabidopsis* and rice FAMA, there are differences in the arrest phenotype of *Arabidopsis* and rice *fama* mutants. Most notably, *osfama-1* mutants do not produce excess tumor-like cells in the stomatal cell rows. One plausible explanation for this difference is tied to the difference in stomatal lineage ontogeny. In *Arabidopsis*, GMCs differentiate from continuously (asymmetrically) dividing meristemoid cells and must change their division program to undergo a single symmetric division to form the guard cell pair. In grasses, GMC formation is one of the earlier stages in development and is succeeded by the recruitment of subsidiary mother cells (SMCs) from neighboring cell files. Therefore, grass GMCs are less transient cell types and are involved in several important signaling steps before they differentiate into guard cells. Rice GMCs might have intrinsically different cell cycle control features that have already acted to prevent excessive GMC division upstream of *OsFAMA* activity.

MUTE and SPCH functions might have diverged

SPCH and *MUTE* control the initiation and termination of the stem cell-like meristemoids (MacAlister et al., 2007; Pillitteri et al., 2007). In the expression and functional studies on the rice and maize homologs of these genes, we found some evidence for their conserved roles in stomatal development; however, there were also some significant differences. Overexpression of *OsSPCH* could induce ectopic cell divisions and *osspch2-1* mutants have fewer stomata than do wild type [similar to the phenotype of the weak

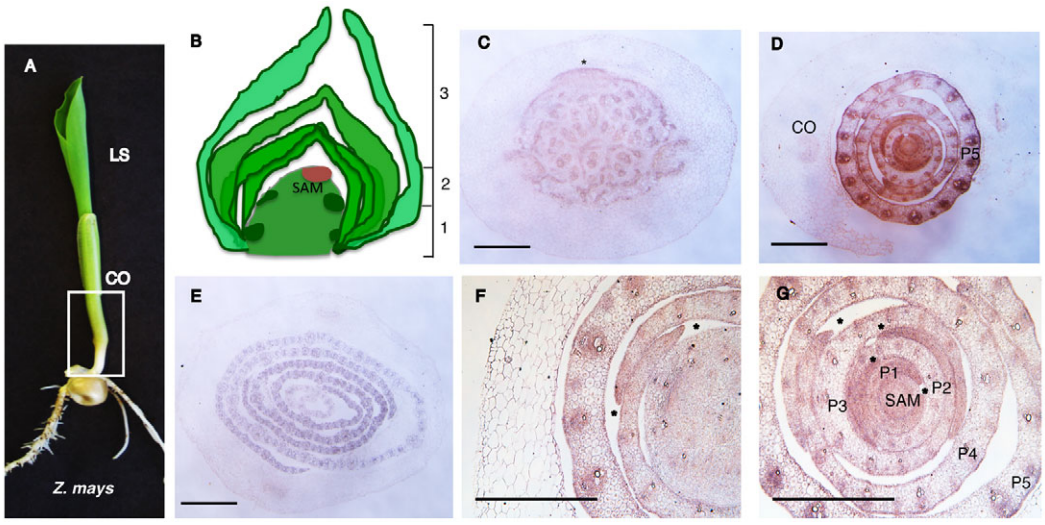

Fig. 9. RNA expression pattern of *ZmMUTE* during early maize leaf development. (**A**) 5-dpg wild-type maize seedling; region diagramed in B is boxed. CO, coleoptile; LS, leaf sheath. (**B**) Maize meristem with height of transverse sections indicated as 1-3. (**C**) Cross section through the vegetative maize apex at height 1. *ZmMUTE* is weakly expressed in the P1 primordium (asterisk). (**D**) Cross section through the SAM at height 2, showing *ZmMUTE* in the SAM and the epidermis of P1 to P5. (**E**) Cross section of maize apex at height 3, showing transcripts in the epidermis of older leaves. (**F**) Higher magnification images of cross section at height 1, showing strong expression in the epidermis and leaf margins, but not in the coleoptile. (**G**) Close-up of cross section through the SAM, showing *ZmMUTE* in the SAM and strong expression in the leaf margins. Asterisks indicate stronger expression at the leaf margins. Scale bars: 50 μm in C-E; 100 μm in F,G.

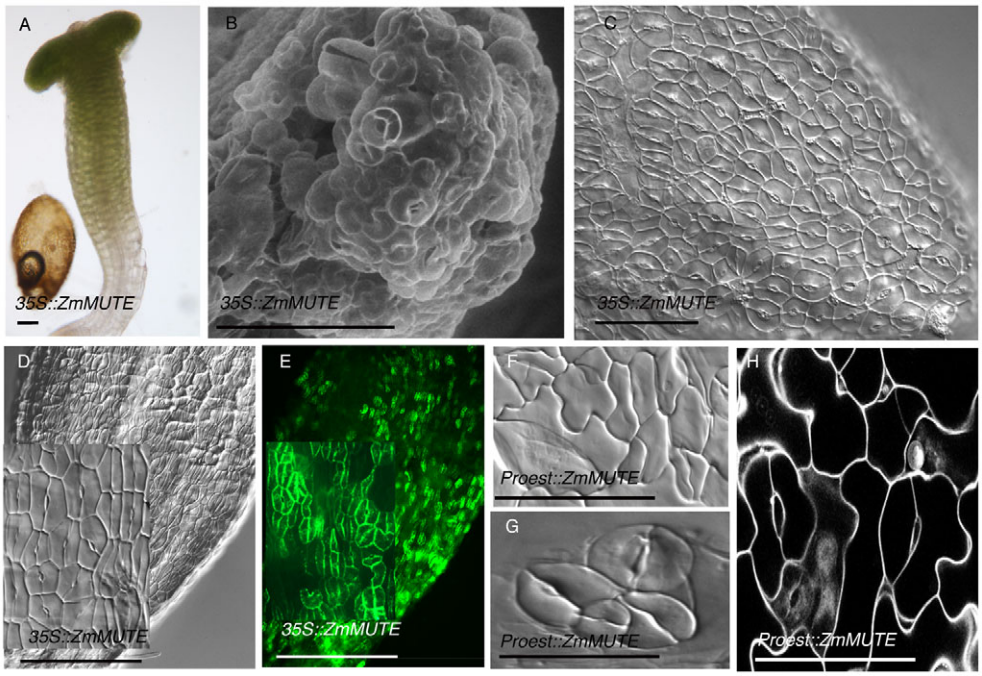

Fig. 10. Phenotypes of *Arabidopsis* seedlings expressing *35S:ZmMUTE*. (**A**) Overall morphology of an *Arabidopsis 35S::ZmMUTE* transgenic seedling. (**B**) Scanning electron microscope image of a *35S::ZmMUTE* cotyledon showing excessive stomatal production. (**C**,**D**) DIC images of cotyledon (C) and hypocotyl (D) in *35S::ZmMUTE* plants. Inset in D is a higher magnification of the hypocotyl region to show excessive stomatal production. (**E**) Expression pattern of the guard cell marker E1728::GFP (green) in the hypocotyl and root region of a *35S::ZmMUTE* seedling; inset is at higher magnification to show guard cell morphology. (**F-H**) Stomatal clusters and conversion of pavement cells into stomata produced by the induction of Pro_{Est}*::ZmMUTE*. Scale bars: 100 μm in B,C,F-H; 50 μm in D,E.

spch-2 allele (MacAlister et al., 2007)], suggesting that SPCH has a general role in promoting early lineage cell divisions. However, OsSPCH2 was not capable of complementing *spch*, indicating that cell fate promoting roles might have diverged.

Both OsMUTE and ZmMUTE are expressed during stages in which the stomatal cell files are forming, suggesting that MUTE acts at an earlier stage of stomatal development in grasses than in *Arabidopsis*. Consistent with these findings, a GUS reporter driven by *OsMUTE* 5′ regulatory regions in *Arabidopsis* exhibited an *SPCH*-like expression pattern in young leaves. Although both *ZmMUTE* and *OsMUTE* can partially complement *mute*, their overexpression phenotypes are substantially different than that of *MUTE*. Expression of *35S::OsMUTE* in an *spch* background allowed us to uncouple cell division from cell fate promotion. In plants with no stomatal lineage, *MUTE* can drive cells to a GMC (and later stomatal) fate; however, *OsMUTE* produces primarily cell divisions, a phenotype that is not only different from that of *MUTE*, but which in fact resembles the phenotypes produced by MPKTD-altered variants of SPCH (Lampard et al., 2008).

Divergent behavior of MUTE homologs might be expected if we consider the developmental events that precede stomatal formation in dicots and monocots. In *Arabidopsis*, it appears that any protodermal cell is capable of undergoing asymmetric stomatal lineage-forming divisions. Mitotic activity is not limited to a specific spatiotemporal domain and stomatal lineage cells act as dispersed ‘stem cell-like’ populations. By contrast, monocots exhibit a very orderly and directional pattern of stomatal development and do not utilize stem cell-like divisions (Stebbins, 1960). The functions of SPCH and MUTE in *Arabidopsis* are tied to the initiation and termination of the stem cell-like divisions in meristemoids. In the grasses, a SPCH-like function (initiating asymmetric divisions) happens with MUTE-like timing (immediately preceding GMC formation), therefore the activity of OsMUTE could be reasonably hypothesized to be a hybrid between that of *Arabidopsis* SPCH and MUTE (Fig. 11).

These hypotheses are useful for considering the difference between monocots and dicots; however, we also see differences in the behavior of MUTE between the two monocots. Distinctive

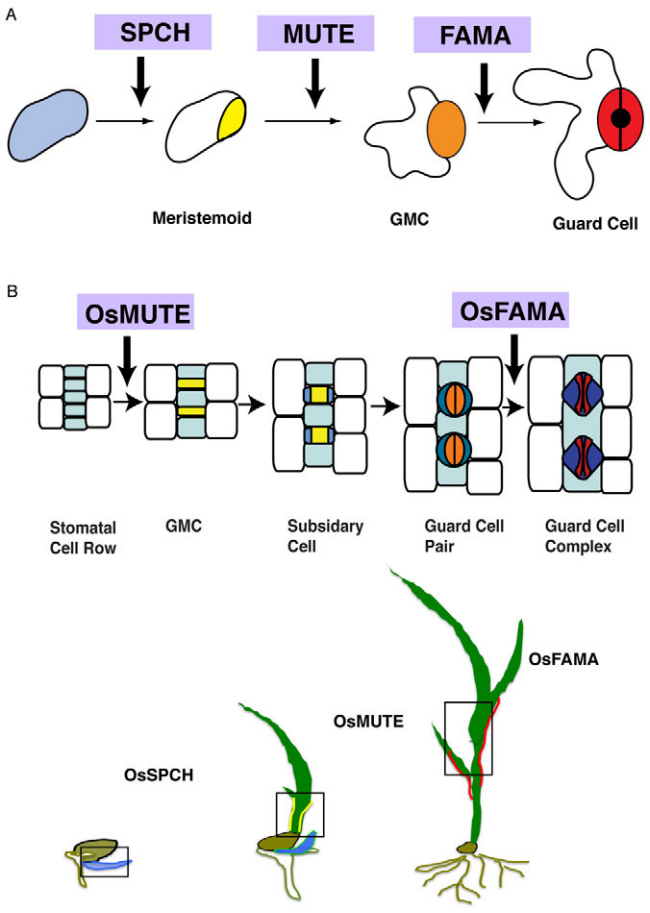

Fig. 11. Model for bHLH proteins in stomatal formation. (**A**,**B**) Schematics comparing stomata formation in *Arabidopsis* (A) and rice (B), indicating the proposed sites of action of SPCH, MUTE and FAMA. We propose that SPCH homologs in the grasses would act before the stages represented in this stomatal lineage diagram.

behaviors of rice and maize MUTE again could reflect differences in the MUTE proteins or in leaf development between the two grass species. *ZmMUTE* contains HBD and HTH domains that often mediate the dimerization of DNA-binding regulatory proteins (Kwok et al., 1999), and a PTB domain known to function as an adaptor to organize signaling complexes (George et al., 2008). However, no predicted protein-interaction domains are found in *OsMUTE*. It might be that *MUTE* is required to interact with partners in maize (and *Arabidopsis*), but not in rice. In terms of leaf development, rice leaf primordia initiate only after the prior two leaves extend, producing a shoot apex with no more than three developing leaves at a given time. Maize produces leaf primordia more rapidly, so that at least five developing leaves are always apparent at the shoot apex (Sylvester et al., 2001). If *MUTE* is required during specific time periods when the stomatal lineage is initiating, then the different leaf initiation rates in the two grasses might require different levels or activities of *MUTE*.

Understanding how *SPCH*, *MUTE* and *FAMA* behave also requires a consideration of their potential partners. In *Arabidopsis*, *SCREAM* (*SCRM*; also known as *ICE1*) and *SCRM2*, are required for multiple stages in stomatal development and might act by forming heterodimers with *SPCH*, *MUTE* and *FAMA* (Kanaoka et al., 2008). The presence of rice genes with significant similarity to *SCRM* (Os11g32100) and *SCRM2* (Os01g71310) implies that modules for the transcriptional regulation of stomatal development could be conserved. Additionally, the conserved MPKTD in *OsSPCH1/2* and *ZmSPCH1/2* indicates that post-translational regulation of the bHLHs by MAPKs might be widespread.

The details of monocot stomata developmental pathways remain to be elucidated, but can benefit from comparison to the better characterized networks in *Arabidopsis*. Some aspects of grass stomatal development, such as the recruitment of subsidiary cells, however, are not accessible through comparison with *Arabidopsis*. In the future, generating targeted knockouts of grass genes whose homologs were identified in *Arabidopsis*, as well as forward genetic screens in the grasses will be invaluable in defining the elements that create and pattern stomata.

We thank Drs Kathryn Barton and Matthew Evans (Carnegie Institution) for in situ advice and microscopes, Dr Hong-Chang Cui (Florida State University) for *OsSCR1* and Dr Laurie Smith (UCSD) for identifying maize homologs. We are also grateful for stimulating discussions and comments on the work from Drs Vivian Irish and Timothy Nelson (Yale), Dr Jeanette Nadeau (CFU), Dr Virginia Walbot (Stanford) and members of the Bergmann laboratory. This work was supported by NSF-IOS-0544895 and DOE-FG02-06ER15810.

Supplementary material

Supplementary material for this article is available at http://dev.biologists.org/cgi/content/full/136/13/2265/DC1

References

Bergmann, D. C. and Sack, F. D. (2007). Stomatal development. *Annu. Rev. Plant. Biol.* **58**, 163-181.

Campbell, D. H. (1881). On the development of the stomata of tradescantia and indian corn. *Am. Nat.* **15**, 761-766.

Clough, S. J. and Bent, A. F. (1998). Floral dip: a simplified method for Agrobacterium-mediated transformation of Arabidopsis Thaliana. *Plant J.* **16**, 735-743.

Croxdale, J. L. (2000). Stomatal patterning in angiosperms. *Am. J. Bot.* **87**, 1069-1080.

Curtis, M. D. and Grossniklaus, U. (2003). A gateway cloning vector set for high-throughput functional analysis of genes in planta. *Plant Physiol.* **133**, 462-469.

Edwards, D., Kerp, H. and Hass, H. (1998). Stomata in early land plants: an anatomical and ecophysiological approach. *J. Exp. Bot.* **49**, 255-278.

Evert, R. F. (2006). *Esau's Plant Anatomy: Meristems, Cells, and Tissues of the Plant Body: Their Structure, Function, and Development*. Hoboken, NJ: Wiley-Interscience.

Feller, A., Hernandez, J. M. and Grotewold, E. (2006). An ACT-Like domain participates in the dimerization of several plant basic-helix-loop-helix transcription factors. *J. Biol. Chem.* **281**, 28964-28974.

Garland, R. U. (1984). Cuticular anatomy of angiosperm leaves from the lower cretaceous potomac group. I. zone I leaves. *Am. J. Bot.* **71**, 192-202.

George, R., Schuller, A. C., Harris, R. and Ladbury, J. E. (2008). A phosphorylation-dependent gating mechanism controls the SH2 domain interactions of the Shc adaptor protein. *J. Mol. Biol.* **377**, 740-747.

Kamiya, N., Itoh, J., Morikami, A., Nagato, Y. and Matsuoka, M. (2003). The SCARECROW gene's role in asymmetric cell divisions in rice plants. *Plant J.* **36**, 45-54.

Kanaoka, M. M., Pillitteri, L. J., Fujii, H., Yoshida, Y., Bogenschutz, N. L., Takabayashi, J., Zhu, J. K. and Torii, K. U. (2008). SCREAM/ICE1 and SCREAM2 specify three cell-state transitional steps leading to Arabidopsis stomatal differentiation. *Plant Cell* **20**, 1775-1785.

Kubo, M., Udagawa, M., Nishikubo, N., Horiguchi, G., Yamaguchi, M., Ito, J., Mimura, T., Fukuda, H. and Demura, T. (2005). Transcription switches for protoxylem and metaxylem vessel formation. *Genes Dev.* **19**, 1855-1860.

Kumar, S., Tamura, K. and Nei, M. (1994). MEGA: molecular evolutionary genetics analysis software for microcomputers. *Comput. Appl. Biosci.* **10**, 189-191.

Kwok, S. F., Staub, J. M. and Deng, X. (1999). Characterization of two subunits of Arabidopsis 19S proteasome regulatory complex and its possible interaction with the COP9 complex. *J. Mol. Biol.* **285**, 85-95.

Lampard, G. R., Macalister, C. A. and Bergmann, D. C. (2008). Arabidopsis stomatal initiation is controlled by MAPK-mediated regulation of the bHLH, SPEECHLESS. *Science* **322**, 1113-1116.

Long, J. and Barton, M. (1998). The development of apical embryonic pattern in Arabidopsis. *Development* **125**, 3027-3035.

MacAlister, C. A., Ohashi-Ito, K. and Bergmann, D. C. (2007). Transcription factor control of asymmetric cell divisions that establish the stomatal lineage. *Nature* **445**, 537-540.

Ohashi-Ito, K. and Bergmann, D. (2006). *Arabidopsis* FAMA controls the final proliferation/differentiation switch during stomatal development. *Plant Cell* **18**, 2493-2505.

Pillitteri, L. J., Sloan, D. B., Bogenschutz, N. L. and Torii, K. U. (2007). Termination of asymmetric cell division and differentiation of stomata. *Nature* **445**, 501-505.

Pillitteri, L. J., Bogenschutz, N. L. and Torii, K. U. (2008). The bHLH Protein, MUTE, controls differentiation of stomata and the hydathode pore in Arabidopsis. *Plant Cell Physiol.* **49**, 934-943.

Sack, F. D. (1994). Structure of the stomatal complex of the monocot Flagellaria indica. *Am. J. Bot.* **81**, 339-344.

Stebbins, G. L. (1960). Developmental studies of cell differentiation in the epidermis of monocotyledons. 1 I. Allium, Rhoeo, and Commelina. *Dev. Biol.* **2**, 409.

Sylvester, A. W., Parker-Clark, V. and Murray, G. A. (2001). Leaf shape and anatomy as indicators of phase change in the grasses: comparison of maize, rice, and bluegrass. *Am. J. Bot.* **88**, 2157-2167.

Table S1. Protein identities in bHLH domains among *Arabidopsis*, rice and maize bHLHs

Gene	*AtFAMA*	*OsFAMA*	*ZmFAMA*	*AtMUTE*	*OsMUTE*	*ZmMUTE*	*AtSPCH*	*OsSPCH1*	*ZmSPCH1*	*OsSPCH2*	*ZmSPCH2*
AtFAMA	ID	0.94	0.92	0.75	0.75	0.81	0.75	0.73	0.71	0.75	0.75
OsFAMA	–	ID	0.98	0.77	0.77	0.83	0.73	0.73	0.69	0.73	0.73
ZmFAMA	–	–	ID	0.77	0.75	0.81	0.71	0.71	0.67	0.71	0.71
AtMUTE	–	–	–	ID	0.90	0.92	0.79	0.77	0.77	0.81	0.81
OsMUTE	–	–	–	–	ID	0.92	0.73	0.75	0.75	0.79	0.79
ZmMUTE	–	–	–	–	–	ID	0.75	0.73	0.73	0.77	0.77
AtSPCH	–	–	–	–	–	–	ID	0.83	0.88	0.92	0.92
OsSPCH1	–	–	–	–	–	–	–	ID	0.92	0.92	0.92
ZmSPCH1	–	–	–	–	–	–	–	–	ID	0.96	0.96
OsSPCH2	–	–	–	–	–	–	–	–	–	ID	1
ZmSPCH2	–	–	–	–	–	–	–	–	–	–	ID

ID, identical.

Table S2. Overall protein identities among *Arabidopsis*, rice and maize stomatal bHLHs

Gene	*AtFAMA*	*OsFAMA*	*ZmFAMA*	*AtMUTE*	*OsMUTE*	*ZmMUTE*	*AtSPCH*	*OsSPCH1*	*ZmSPCH1*	*OsSPCH2*	*ZmSPCH2*
AtFAMA	ID	0.27	0.33	0.37	0.34	0.39	0.19	0.17	0.19	0.19	0.22
OsFAMA	–	ID	0.56	0.16	0.18	0.17	0.16	0.17	0.16	0.18	0.18
ZmFAMA	–	–	ID	0.19	0.19	0.19	0.17	0.19	0.20	0.18	0.19
AtMUTE	–	–	–	ID	0.49	0.55	0.21	0.17	0.20	0.20	0.24
OsMUTE	–	–	–	–	ID	0.61	0.20	0.19	0.23	0.23	0.26
ZmMUTE	–	–	–	–	–	ID	0.22	0.19	0.22	0.22	0.25
AtSPCH	–	–	–	–	–	–	ID	0.23	0.28	0.28	0.30
OsSPCH1	–	–	–	–	–	–	–	ID	0.48	0.37	0.35
ZmSPCH1	–	–	–	–	–	–	–	–	ID	0.44	0.43
OsSPCH2	–	–	–	–	–	–	–	–	–	ID	0.60
ZmSPCH2	–	–	–	–	–	–	–	–	–	–	ID

ID, identical.